Received: 25 March 2023 | Revised: 8 June 2023 | Accepted: 3 July 2023

DOI: 10.1002/lio2.1116

ORIGINAL RESEARCH

Laryngoscope Investigative Otolaryngology

First evaluation of an ovine training model for sialendoscopy

Urs Borner MD[1,2] | Marco Caversaccio MD[1] | Franca Wagner MD[3] | Francis Marchal MD[2,4] | Lukas Anschuetz MD[1]

[1]Department of Otorhinolaryngology – Head and Neck Surgery, Inselspital, Bern University Hospital and University of Bern, Bern, Switzerland

[2]European Sialendoscoy Training Center, Geneva, Switzerland

[3]Department of Diagnostic and Interventional Neuroradiology, Inselspital, University Hospital Bern and University of Bern, Bern, Switzerland

[4]Department of Otolaryngology – Head and Neck Surgery, University Hospitals of Geneva, Geneva, Switzerland

Correspondence
Urs Borner, Department of Otorhinolaryngology – Head and Neck Surgery, Inselspital, University Hospital Bern, 3010 Bern, Switzerland.
Email: urs.borner@insel.ch

Funding information
SWF (Stiftung für wissenschaftliche Forschung)

Abstract

Objective: Sialendoscopy is a minimally invasive diagnostic and therapeutic technique used in the treatment of various salivary gland diseases. To date, there are very few suitable training models other than the pig's head, which has been used at the European Sialendoscopy Training Center for 22 years. The goal of this study was to describe an ovine model for sialendoscopy training and compare the ovine model's to the human anatomy. We propose a step-by-step approach for sialendoscopy training using this ex-vivo model.

Methods: The anatomy of the ovine salivary ducts and glands was assessed by magnetic resonance imaging using one fresh ovine head. Thereafter, the model was designed during dissection by an experienced sialendoscopist. The various steps were then validated during consecutive dissections using a Likert-scale questionnaire.

Results: The full model was described in the form of a dissection guide and allowed reliable diagnostic sialendoscopy in 10/10 Stenson's and in 5/10 Wharton's ducts. Moreover, interventional sialendoscopy was simulated to provide a training model for the removal of sialoliths in the Stenson's duct. The human and ovine anatomy are quite similar allowing a training experience close to reality.

Conclusion: We developed and evaluated an ovine model with the goal of improving training in diagnostic and interventional sialendoscopy. In particular, the Stenson's duct can be successfully prepared, probed and subjected to sialendoscopy. The realistic anatomical environment and excellent tissue quality created a life-like training experience for an experienced sialendoscopist. Further studies with beginners are necessary to validate this model as a training model.

Level of Evidence: 4.

KEYWORDS
ovine model, salivary gland, salivary stone, sheep, sialendoscopy, training model

1 | INTRODUCTION

Technical innovations and advances in endoscopic technologies led to the introduction of sialendoscopy. Sialendoscopy with a nude optic fiber was first described by Katz et al.[1] and Königsberger et al. in 1990.[2] Nahlieli et al. described sialendoscopy and basket retrieval with the use of a rigid endoscope in the mid-1990s.[3] The development of a minimal invasive approach was finally developed and promoted by Marchal et al.[4]

It offered a new procedure for visualizing the salivary ducts and treating diseases of them with a minimally invasive approach and associated instrumentation.[4,5] Another advantage is that the procedure can usually be performed under local anesthesia.[6] Consequently, it has been adopted worldwide and is attracting increasing interest as well as an extending list of indications. Initially, its field of application was salivary stones.[7,8] Later it was shown that salivary duct stenosis can be treated similarly.[9,10] Moreover, sialendoscopy plays a central role in the treatment of juvenile recurrent parotitis.[11–13] In recent years, it has also been applied in patients with Sjögren's syndrome,[14–16] after prostate-specific membrane antigen treatment[17] and when multiple salivary glands are affected.[18]

However, the sialendoscopic approach is technically demanding and is associated with a steep learning curve. Moreover, the fact that the interventions can be performed under local anesthesia limits training opportunities. Therefore, it is important to design and develop low-cost models for education and training outside the operating room. Such models need to be suitable for enabling inexperienced surgeons to learn how to handle the surgical instruments correctly.

In this context, the ovine model has been identified as a possible suitable option for use in training in head and neck endoscopy and salivary gland surgery.[19–22] The anatomical structures correspond to the human anatomy in terms of size and tissue consistency. In addition, sheep's heads are available inexpensively and ubiquitously as slaughterhouse waste.

We therefore hypothesized that the ovine model would be suitable for sialendoscopy simulation and training. The aims of the present study are:

- To describe and investigate the feasibility of using the sheep's head as an ex-vivo model by comparing the ovine to the human anatomy.
- To outline a step-by-step approach and a dissection guide for sialendoscopy training.

2 | MATERIALS AND METHODS

We started by performing magnetic resonance imaging (MRI) on one fresh sheep's head using a 3 T imaging system (Prisma, Siemens Medical Solutions, Nürnberg, Erlangen, Germany). A specified imaging protocol was followed to investigate the salivary glands, including a 3D T2 SPACE weighted (w) sialo-MRI sequence with a slice thickness of 1 mm, a 3D T2w SPACE SPAIR with a slice thickness of 0.6 mm and a coronal T2w STIR to visualize the salivary ducts. The parameters for the 3D T2 SPACE sequence were: repetition time (TR) 3200 ms; time to echo (TE) 381 ms; slice thickness 1.0 mm; field of view (FOV) 256 × 256 mm; and acquisition time 5:16 min. The parameters for the 3D T2w SPACE SPAIR were as follows: TR 1200 ms; TE 178 ms, slice thickness 0.6 mm; FOV 200 × 200 mm; and an acquisition time of 6:18 min.

The coronal T2w STIR was scanned with a TR 6810 ms; TE 62 ms; slice thickness 3.0 mm; FOV 280 × 280 mm; and an acquisition time of 4:12 min.

Based on the insights gained into ovine anatomy the model was progressively developed during repeated dissection of fresh lamb's heads. From the experiences of the European Sialendoscoy Training Center, Geneva, Switzerland with pig's heads, we know that the cadavers must be fresh to offer the best quality for use as a model. Standard surgical equipment and a saw was used to prepare the specimen.

Sialendoscopy was performed by an experienced surgeon using Marchal all-in-one sialendoscopes 1.3 coupled to high-definition video and camera equipment (Karl Storz, Tuttlingen, Germany). The lamb's heads were from animals slaughtered for alimentary use and were acquired from the local butcher. Agricultural and veterinary well-being of the animals is subject to local regulations.

Dissection of the salivary gland system was performed on 10 sides (5 heads). The anatomy assessed and the model for sialendoscopy we developed are described below. During the preparation of the 1st, 5th and 10th sheep's head, the time necessary for the dissection was recorded.

2.1 | Step-by-step dissection guide

A. Preparation of the model

- Make a skin incision from the parotid gland to the snout (white line in Figure 1A).
- Raise the subcutaneous skin flaps cranially and caudally (Figure 1B) and identify and dissect the superficial musculoaponeurotic system (SMAS).
- Resect the skin (Figure 1C).
- Saw through the maxilla, 7 cm from the snout (Figure 1D).

B. Dissection of Stenson's duct

- Make horizontal cuts—buccal caudal and cranial (white lines)—to remove the lips (Figure 2A).
- Identify the papilla of Stenson's duct (Figure 2B): 2 cm anterior to the border of the masseter muscle (Figure 2C) and opposite the upper second molar tooth.
- Dilate the papilla with the dilator (Figure 2C) and the conic dilator (Figure 2D).

C. Dissection of Wharton's duct

- Fix the tongue to the lateral wall of the nose (Figure 2E).
- Locate the caruncula, which is found at the beginning of the salivary crest, 3 mm from the midline, as shown by the white arrow in Figure 2F.

D. Sialendoscopy

- The sialendoscope is very fragile: make sure to handle the equipment with the utmost care. After removing it from the container, the light source must be connected.

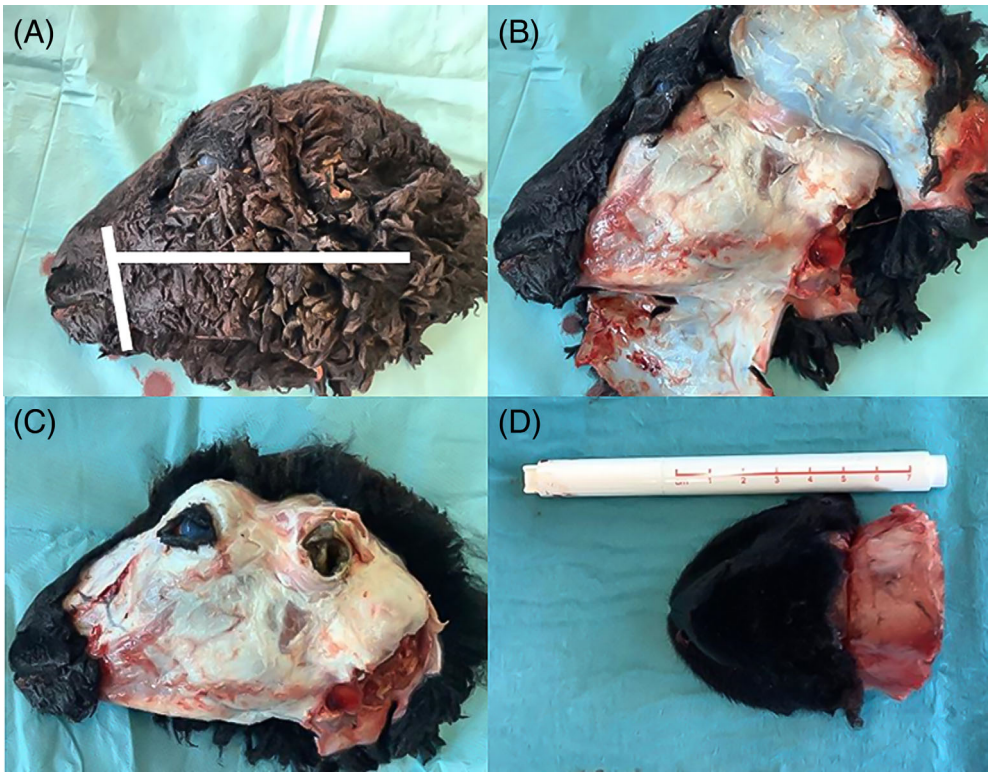

FIGURE 1 Preparation of the sheep's head. (A) Incision from the parotid gland to the snout. (B) Raise the subcutaneous skin flaps cranially and caudally and identify and dissect the superficial musculoaponeurotic system (SMAS). (C) Resect the skin. (D) Saw through the maxilla, 7 cm from the snout.

- Use saline solution for rinsing. This is administered to the sialendoscope via a 20 mL syringe through a tube.
- Remove the protective cover from the sialendoscope.
- First, the horizon must be set and the image quality adjusted. Finally, the white balance is adjusted.
- Dilate Stenson's duct with dilators and probes (Figure 2C).
- Dilate Wharton's duct with dilators and probes (Figure 2G).
- Introduce the 1.3 mm all-in-one sialendoscope into the Stenson's duct (Figure 3A).
- Rinse with saline solution.
- Perform endoscopy of Stenson's (Figure 3B) and Wharton's duct (Figure 3C).

E. Retropapillary approach (Figure 3D)

- Make an incision of 3 cm on the salivary crest.
- Dissect and identify Wharton's duct.
- Open the duct and introduce the endoscope (Figure 3E).

F. Model of interventional sialendoscopy

- Make an incision in the area of the middle third of Stenson's duct, above the masseter muscle (Figure 3F) and insert a rice grain.
- Close the Stenson's duct with a non-absorbable suture.
- Introduce the endoscope, rinse, and perform sialendoscopy upon identifying the rice grain inside the duct.
- The foreign body in Stenson's duct is shown by an arrow in Figure 4A.
- Catch the foreign body using a 4-wire stone extractor (Karl Storz) as depicted in Figure 4B,C. An endoscopic view of the stone extractor and the captured foreign body is shown in Figure 4D.

2.2 | Subjective validation

During testing of the model, its suitability was rated by the experienced sialendoscopy surgeon after every intervention with respect to five dimensions: tissue quality, reproducibility of the surgical scenario, comparison with a real-life scenario (in the operating theater), subjective learning effect rated by the operating surgeon after the training, and overall rating. We used a rating scale ranging from 1 (very poor) to 10 (excellent).

3 | RESULTS

3.1 | Magnetic resonance imaging

Based on the MRI of one sheep's head we visualized the salivary glands and the ductal system using the same imaging protocol as we use in humans with suspected disease of the salivary duct system. The sheep's parotid glands can be visualized behind the mandible and have the same density as in humans. The submandibular glands, which are located at the inferior border of the mandible, are smaller in sheep

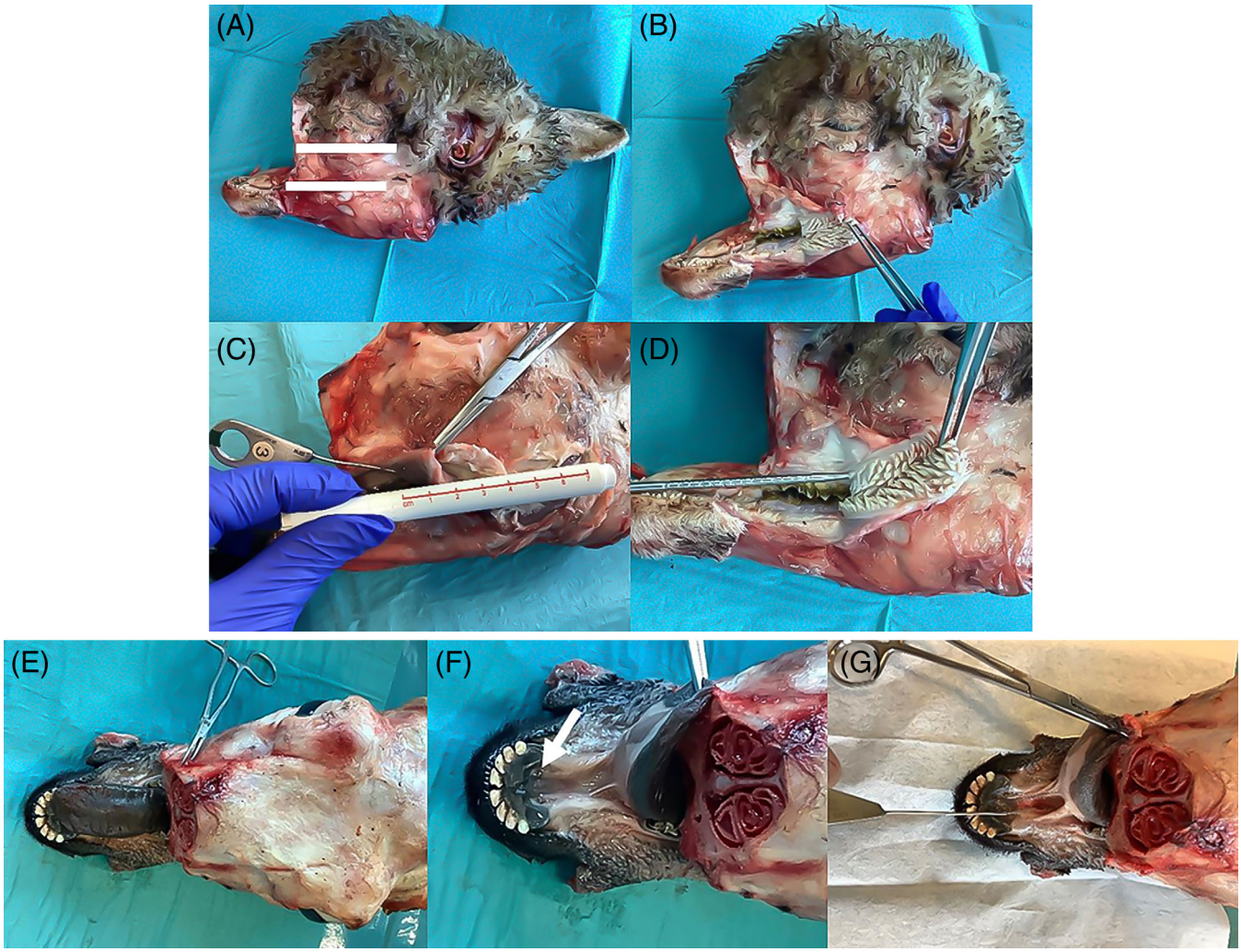

FIGURE 2 Access to the salivary ducts (ducts access and access 2). (A) Make horizontal cuts—buccal caudal and cranial (white lines)—to remove the lips. (B) Identify the papilla of Stenson's duct. (C) 2 cm anterior to the border of the masseter muscle and opposite the upper second molar tooth. Dilate the papilla with the dilator. (D) Dilate the papilla with the conic dilator. (E) Fix the tongue to the lateral wall of the nose. (F) Locate the caruncula, which is found at the beginning of the salivary crest, 3 mm from the midline as shown by the white arrow.

than in humans. Stenson's duct can be completely visualized on both sides (Figure 5C,D). At a distance of 3 cm from the papilla we observed the kinking of the duct on both sides (Figure 5C,D arrow). Wharton's duct is so narrow that it cannot be imaged along its entire length (Figure 5C star). The comparative anatomy of the salivary ducts is summarized in Table 1.

3.2 | Glandular anatomy (preparation of the model)

After dissection of the skin flaps as described above, the SMAS was displayed and dissected. The salivary glands and ducts were then dissected and skeletonized. In the sheep, the parotid gland is located between the mandible and the external auditory canal. Its volume is approximately 12 cm^3. The submandibular gland is located in the submandibular space. Both major salivary glands are located in the same place in sheep as in humans.

3.3 | Ductal anatomy (dissection of the ducts)

The ovine parotid duct exits the gland at its ventral and rostral surface coursing along the ventral and rostral border of the masseter muscle, as it is located between the muscle and the facial vein. It enters the oral cavity opposite the upper second molar tooth.[23] This course in the sheep is anatomically very similar to that in humans. However, it is narrower and the extraparenchymal part is significantly longer, with a maximal length of up to 9.5 cm compared to approximately 4–6 cm in humans. Also, the sheep's parotid duct does not run completely horizontally but curves downward to the parotid gland. Wharton's duct runs around the mylohyoid muscle. The submandibular glands are very small in the sheep, with a correspondingly much narrower Wharton's duct (probe 4) than in humans (probe 6). The caruncula can be easily localized, but dilatation is only possible up to probe 4. A summary of the comparative anatomy is provided in Table 1.

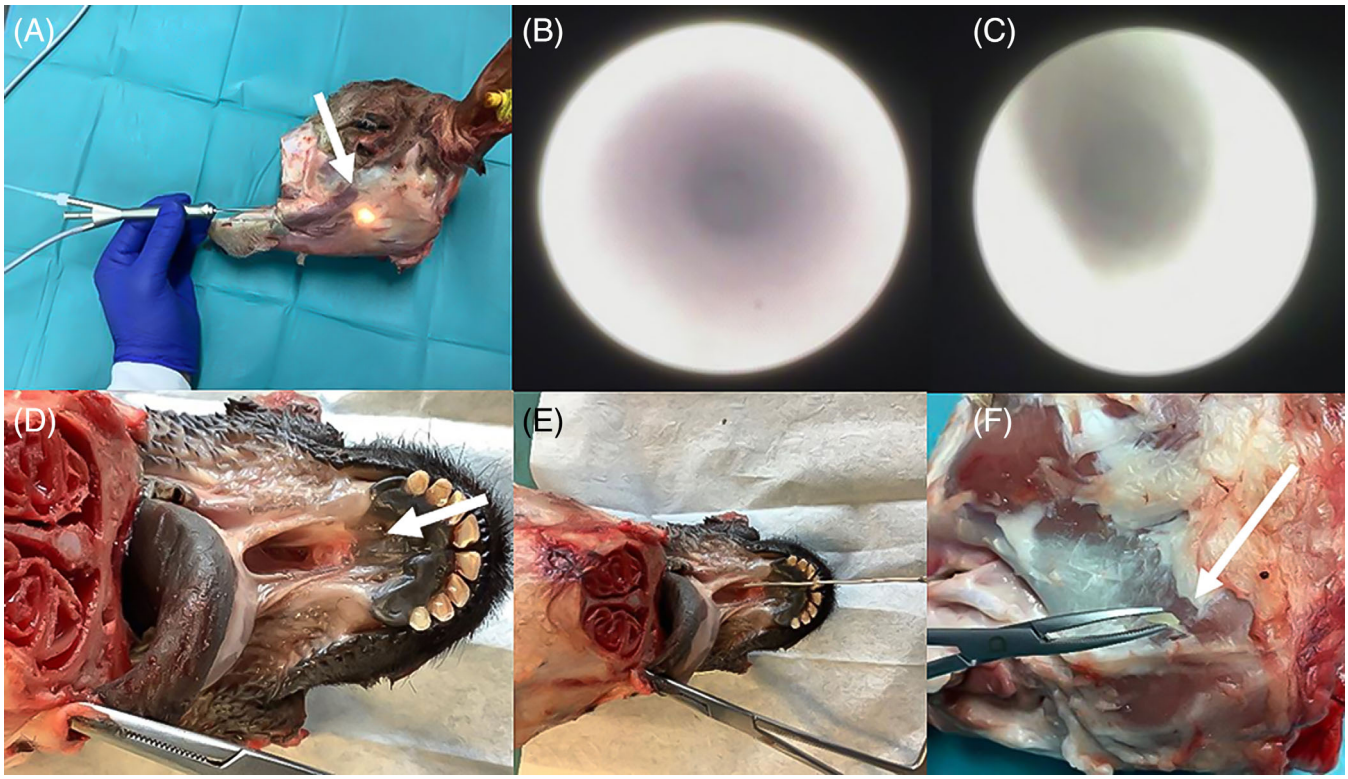

FIGURE 3 Sialendoscopy of Stenson's duct. (A) Introduce the 1.3 mm all-in-one sialendoscope into the Stenson's duct. Perform endoscopy of Stenson's (B) and Wharton's duct (C). (D) Retropapillary approach. (E) Make an incision of 3 cm on the salivary crest. Dissect and identify Wharton's duct. Open the duct and introduce the endoscope. F: Make an incision in the area of the middle third of Stenson's duct, above the masseter muscle, and insert a rice grain. Introduce the endoscope, rinse, and perform sialendoscopy upon identifying the rice grain inside the duct.

3.4 | Comparative sialendoscopic anatomy

The endoscopic anatomy of the ovine Stenson's duct is similar to that in humans. The endoscopic anatomy of ovine Wharton's duct was onlyaccessible in 5/10 cases and only the first 2 cm could be endoscoped with the 1.3 mm sialendoscope (Table 1).

- Stenson's duct: A kink in the duct occurs after a mean distance of 3.1 cm (range: 2.8–3.4 cm), which is related to the crossing of the masseter muscle. It can be overcome by rinsing with liquid. Sialendoscopy of the duct can be performed up to 9.5 cm. The outer diameter of the duct is 4 mm and the inner diameter is 2.5 mm.
- Wharton's duct: Using a 1.3 mm sialendoscope, sialendoscopy can only be performed up to 2 cm. After that, the duct is too narrow to go any further.

3.5 | Endoscopic results

Sialendoscopy was performed in 10 Stenson's ducts in 5 sheep's heads:

- Stenson's duct could be dilated and examined by sialendoscopy in all cases.

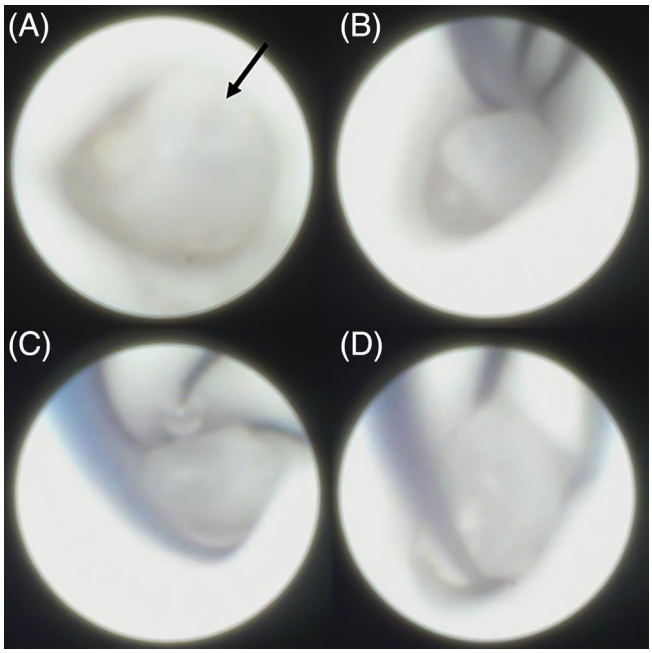

FIGURE 4 Sialendoscopic removal of a grain of rice. (A) The foreign body in Stenson's duct is shown by an arrow. (B, C) Catch the foreign body using a 4-wire stone extractor (Karl Storz). (D) An endoscopic view of the stone extractor and the captured foreign body.

- Applying our model of interventional sialendoscopy we were able to simulate the removal of a foreign body from the Stenson's duct using a stone extractor (4-wire basket; outer diameter, 0.4 mm; Karl Storz [Figure 4]).

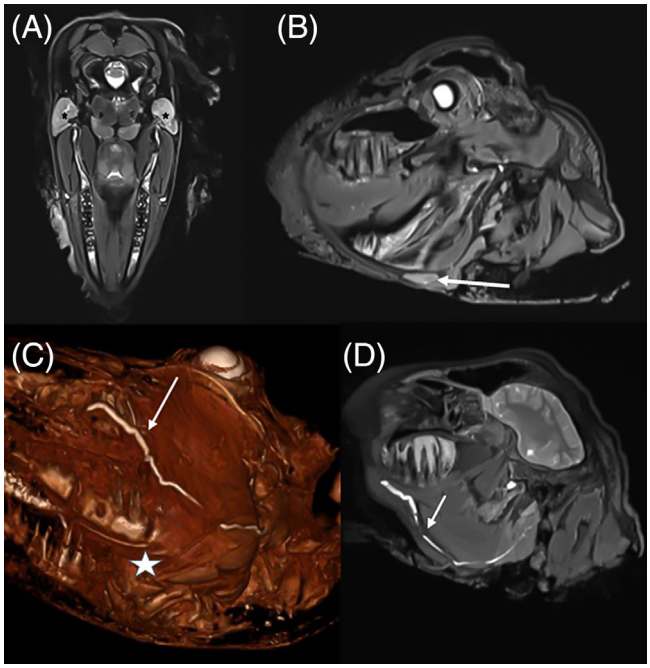

FIGURE 5 Sialo-MRI of sheep's head. (A) Parotid glands and the ductal system. (B) The submandibular gland (arrow) and the ductal system. Wharton's duct is so narrow that it cannot be imaged alongits entire length. (C) The submandibular gland (star), which is located at the inferior border of the mandible, is smaller in sheep than in humans. (C) Stenson's duct can be completely visualized (arrow). (D) At a distance of 3 cm from the papilla we observed the kinking (arrow) of the duct on both sides.

Sialendoscopy was performed in 10 Wharton's ducts in 5 sheep's heads:

- In five cases the caruncula was too small and rigid to be dilated and a retropapillary approach was necessary.
- During diagnostic sialendoscopy, via retropapillary access, it was possible to access the duct with the 1.3-mm sialendoscope in all cases. However, due to the size of the sialendoscope, it was only possible to sialendoscope the first 2 cm.

3.6 | Surgical results

As expected, the time required for dissection decreased over the course of the successive sessions and there was a continuous reduction in the time needed to accomplish the individual surgical steps. The preparation of the skin took 6.3 min (standard deviation (SD): 2.9) per side. The mean time needed to prepare the nose was 10 min (SD: 4.1), and, to prepare the papilla, 6 min (SD: 4.3) were required per side. For dilation of the papilla on both sides the mean time needed was 3.3 min (SD: 0.5).

3.7 | Subjective feedback

Subjective feedback was collected after each of the dissections and scores were reported as mean with SD. Mean values for the different aspects were: tissue quality, 8.4 (SD: 1.1); reproducibility of the

TABLE 1 Comparative anatomy of dissection and sialendoscopy.

	Human		Ovine	
	MRI	Anatomy	MRI	Anatomy
Stenson's duct				
Over muscle masseter	Yes	Yes	Yes	Yes
Through muscle buccinator	Yes	Yes	Yes	Yes
Diameter (mm)	2.0 (1.9–2.5)	1.4	2.2	Outer 4 mm Inner 2.5 mm
Length (cm)	5.4 (4.2–6.1)	5.8 (4–6)	9.8	9.5 (9–11)
Curved	Yes	Yes	Yes	Yes
Stenosis	In the middle of the duct	In the middle of the duct	After 2 cm	After 3.1 cm
Wharton's duct				
Relationship to the zygomatic arch	1–2 cm inferior	1–2 cm inferior		
Through muscle buccinator	Yes	Yes	Yes	Yes
Diameter (mm)	1.3 (1.0–2.0)	1.5	1.3	Outer 2 Inner 1.3
Length (cm)	5.3 (4.6–5.9)	5.6	4.8	1.5
Curved	Two curves	Two curves	Two curves	Two curves
Stenosis	No	No	No	No

Abbreviation: MRI, magnetic resonance imaging.

surgical situation, 7.8 (SD: 1.3); comparison with real-life scenario, 8 (SD: 0.8); learning effect, 8.8 (SD: 0.9), and the score for the overall evaluation was 9.1 (SD: 0.7). The surgeon found the model very convenient to practice on.

4 | DISCUSSION

Sialendoscopy is a minimally invasive technique used to diagnose and treat salivary gland diseases. Although the technique is technically challenging and is associated with a long and steep learning curve, its advantages are well described. However, there is a lack of possibilities for the training that is required to achieve sufficient proficiency before treating patients, as well as to improve skills with more advanced interventional techniques. For this reason, we investigated the ex-vivo ovine head as a training model for diagnostic and interventional sialendoscopy to see if a model other than the pig's head would be suitable.

4.1 | Comparative anatomy

Dehghani et al. reported the diameter of Stenson's duct in the sheep as 3.1 ± 1 mm and Wharton's duct as 1.4 ± 0.2 mm.[24] Similarly, we measured a mean inner diameter of 2.5 mm for Stenson's duct and 1.2 mm for Wharton's duct in sheep.

Uzun et al. measured the length and course of Stenson's duct during dissection of 13 ovine parotid glands. They found an average length of 10.92 ± 1.02 cm.[23] We observed an average length of 9.5 cm as assessed by sialendoscopy. The difference between these measurements is mainly explained by the different assessment techniques (dissection vs. endoscopy) because, during dissection, parts of the intraglandular duct system were also measured. Another explanation could be the possibility of different breeds and therefore slightly different anatomy.

In the literature, the reported diameter of Stenson's duct in humans is 1.4 mm and that of Wharton's duct is 1.5 mm.[25] The average length of Stenson's duct is 5.8 cm (4–6 cm) and that of Wharton's duct is 5.6 cm.[25] Thus, both ducts are significantly longer in the sheep's head than in humans. The course of both ducts is very similar in sheep and humans, as described in the results section. In our opinion, the longer duct in sheep is an advantage, especially for beginners in the technique, since it allows easier handling of the sialendoscope during practice. In particular, the basket can be handled, and the technique practiced more easily than in humans. Thus, from an anatomical point of view, the ovine model is well suited for training purposes especially for sialendoscopy of the parotid duct.

4.2 | Training model

Successful medical education and training of young surgeons relies essentially on the teaching of intellectual content and manual skills. An important part of this action-oriented teaching involves observation of specialists in the operating room.[26–29] The students observe the procedures and learn the step-by-step approaches and methodology for further hands-on training. At a later stage, by practicing these individual step-by-step approaches under guidance, they slowly improve their manual skills, enabling them to become progressively more proficient and independent surgeons. Currently, this aspect of teaching largely takes place in the operating rooms and depends on the willingness of the operating surgeons to communicate and teach. In times of rising health care costs and scarcity of public funds for medical teaching at university hospitals, an increase in the efficiency of medical education and training is desirable.[30] In particular in the context of minimally invasive procedures, there is, in our opinion, a clear need to increase the training facilities using models. This provision is increasing with the increasing numbers of surgical simulation training centers around the globe. This is particularly important for procedures with long learning curves, especially for the ones performed under local anesthesia. In such cases, the patient might not easily understand why the operation might be long and complicated when a trainee is present. Therefore, a low-cost, reliable and easily available training model is an unmet need in teaching and training in sialendoscopy. Few publications have so far described training models for this purpose.[27,28,31]

Pig's heads have been successfully used at the international sialendoscopy center in Geneva, Switzerland, for more than 20 years. During this time over 1600 physicians have been trained using this model for diagnostic and interventional sialendoscopy (removal of foreign bodies with a basket, dilatation with low and high pressure balloons, and laser fragmentation). Saga-Gutierrez et al. described the use of the pig's head model with omeprazole spheres to simulate lithiasis.[31] Taking a different approach, Robaskewicz Pascoto et al. described a synthetic simulator for training in sialendoscopy. It used a thermo-retractile and thermo-sensible rubber which, when combined with different polymers, is able to simulate more than 30 different textures, consistencies and mechanical resistances.[27]

We consider that the sheep's head has several advantages over the pig's head, including faster and easier preparation. Its smaller size means that transport and disposal are also easier. Moreover, due to cultural differences, pig's heads may not be available in some countries; therefore, the ovine model offers a suitable alternative.

In contrast, the synthetic model is quite complex to use, is not readily available and does not simulate the difficulty for the papilla. Moreover, tissue consistency in our ovine model is lifelike, which is certainly another advantage.

4.3 | Subjective validation

The subjective rating of our model by the first author of this article, an experienced sialendoscopist, indicated excellent tissue quality of the fresh specimens.

Compared to the real-life procedure, the model also performed very well. As expected, the difficulties encountered during the

endoscopy of the sheep's head decreased over the course of operating on the 10 subsequent sides. Probing and preparing the Wharton's duct in all 10 cases was limited by the fact that the duct could only be endoscoped up to 2 cm using the 1.3 sialendoscope. It might have been possible to go much further with a smaller sialendoscope. The overall rating increased over the 10 sessions.

We also developed a simulation for salivary stone removal using rice grains. The insertion of the grain was easily accomplished through an external incision. During endoscopy, the grain could be grasped and removed by means of a basket, as in the real-life procedure. In our opinion, this presents a valuable training opportunity, as hand–eye coordination is usually the most challenging aspect of salivary stone extraction in humans.

It is noticeable that there were large differences in the time taken for preparation of the model as well as a learning curve for skin preparation and for visualization of the duct openings. In contrast, we could not detect any change in the time needed for dilatation of the duct openings. This is most likely because the dilation procedure is very similar to the one used in humans and was performed by an experienced sialendoscopist.

With the detailed step-by-step description of the preparation presented here, we aim to facilitate the application of the ovine model for diagnostic and interventional sialendoscopy and enable its widespread application in postgraduate teaching. Preparation for access is also good practice for the surgeons in training. However, the preparation is time consuming. For this reason, in courses with limited time, the preparation of the sheep heads can also be done in advance. A big advantage of the sheep heads is the transport. The sheep heads can be transported without problems, because they are much smaller and take up less space. This is especially important when several heads are needed. First, however, it will be necessary to assess whether the model is also suitable for beginners.

The study had some limitations. One limitation is that the model was evaluated by an experienced sialendoscopist. It has not yet been validated by a large group of beginners and sialendoscopists, which would be the obvious next step.

Diagnostic sialendoscopy of Wharton's duct using a 1.3 mm endoscope was only possible in 5/10 cases. Via retropapillary access it was possible to endoscope the remaining five ducts. However, due to the size of the sialendoscope, it was only possible to sialendoscope the first 2 cm.

5 | CONCLUSION

We investigated and evaluated the anatomy of the sheep's head by dissection, and the salivary ducts by MRI and by endoscopy in search of a new training model for sialendoscopy. We conclude that in experienced hands, the Stenson's duct is suitable for diagnostic and therapeutic sialendoscopy. A step-by step dissection guide was designed, and its feasibility demonstrated. Further evaluation is needed to show whether the model is suitable for beginners.

AUTHOR CONTRIBUTIONS

Urs Borner, Lukas Anschuetz, Marco Caversaccio and Franca Wagner had the original idea, designed the study and wrote the first draft of the article. Urs Borner and Lukas Anschuetz did the analysis, gave input into the study design and wrote sections of the article. Urs Borner, Lukas Anschuetz, Marco Caversaccio, Franca Wagner and Francis Marchal helped to interpret the results, and wrote sections of the article. The corresponding author attests that all listed authors meet authorship criteria and that no others meeting the criteria have been omitted. Urs Borner is the guarantor.

ACKNOWLEDGMENTS

The authors are grateful for the funding by SWF (Stiftung für wissenschaftliche Forschung).

FUNDING INFORMATION

This study was funded by the SWF (Stiftung für wissenschaftliche Forschung).

CONFLICT OF INTEREST STATEMENT

LA is a consultant for Stryker ENT; the other authors declare that they have no conflicts of interest.

ORCID

Urs Borner https://orcid.org/0000-0003-1186-4181

REFERENCES

1. Katz P. Endoscopy of the salivary glands. *Ann Radiol*. 1991;34(1–2):110-113.
2. Königsberger R, Feyh J, Goetz A, Schilling VKE. Endoscopic controlled laser lithotripsy in the treatment of sialolithiasis. *Laryngorhinootologie*. 1990;69(6):322-323.
3. Nahlieli O, Neder A, Baruchin AM. Salivary gland endoscopy: a new technique for diagnosis and treatment of sialolithiasis. *J Oral Maxillofac Surg*. 1994;52(12):1240-1242.
4. Marchal F, Dulguerov P, Lehmann W. Interventional sialendoscopy. *N Engl J Med*. 1999;341(16):1242-1243. https://pubmed.ncbi.nlm.nih.gov/10523164/
5. Marchal F, Becker M, Dulguerov P, Lehmann W. Interventional sialendoscopy. *Laryngoscope*. 2015;125(11):2427-2429. doi:10.1002/lary.25564
6. Bawazeer N, Carvalho J, Djennaoui I, Charpiot A. Sialendoscopy under conscious sedation versus general anesthesia. A comparative study. *Am J Otolaryngol - Head Neck Med Surg*. 2018;39(6):754-758.
7. Carta F, Farneti P, Cantore S, et al. Sialendoscopy for salivary stones: principles, technical skills and therapeutic experience. *Acta Otorhinolaryngol Ital*. 2017;37(2):102-112. https://pubmed.ncbi.nlm.nih.gov/28516972/
8. Koch M, Mantsopoulos K, Müller S, Sievert M, Iro H. Treatment of sialolithiasis: what has changed? An update of the treatment algorithms and a review of the literature. *J Clin Med*. 2021;11(1):231. https://pubmed.ncbi.nlm.nih.gov/35011971/
9. Koch M, Iro H. Salivary duct stenosis: diagnosis and treatment Stenosi duttali salivari: diagnosi e terapia. *Acta Otorhinolaryngol Ital*. 2017;37:132-141.
10. Choi JS, Choi YG, Kim YM, Lim JY. Clinical outcomes and prognostic factors of sialendoscopy in salivary duct stenosis. *Laryngoscope*. 2018;128(4):878-884.

11. Capaccio P, Sigismund PE, Luca N, Marchisio P, Pignataro L. Modern management of juvenile recurrent parotitis. *J Laryngol Otol*. 2012; 126(12):1254-1260.
12. Leerdam CM, Martin HCO, Isaacs D. Recurrent parotitis of childhood. *J Paediatr Child Health*. 2005;41:631-634.
13. Robbins KT, Woodson GE. Thyroid carcinoma presenting as a parapharyngeal mass. *Head Neck Surg*. 1985;7(5):434-436.
14. Hakki Karagozoglu K, Vissink A, Forouzanfar T, Brand HS, Maarse F, Jan Jager DH. Sialendoscopy enhances salivary gland function in Sjögren's syndrome: a 6-month follow-up, randomised and controlled, single blind study. *Ann Rheum Dis*. 2018;77(7):1025-1031.
15. Gallo A, Martellucci S, Fusconi M, et al. Sialendoscopic management of autoimmune sialadenitis: a review of literature. *Acta Otorhinolaryngol Ital*. 2017;37:148-154.
16. Capaccio P, Canzi P, Torretta S, et al. Combined interventional sialendoscopy and intraductal steroid therapy for recurrent sialadenitis in Sjögren's syndrome: results of a pilot monocentric trial. *Clin Otolaryngol*. 2018 Feb 1;43(1):96-102.
17. Rathke H, Kratochwil C, Hohenberger R, et al. Initial clinical experience performing sialendoscopy for salivary gland protection in patients undergoing 225 Ac-PSMA-617 RLT. *Eur J Nucl Med Mol Imaging*. 2019;46(1):139-147. https://pubmed.ncbi.nlm.nih.gov/30151743/
18. Borner U, Anschuetz L, Caversaccio M, et al. A retrospective analysis of multiple affected salivary gland diseases: diagnostic and therapeutic benefits of interventional sialendoscopy. *Ear Nose Throat J*. 2022: 1455613221081911. https://us.sagepub.com/en-us/nam/open-access-at-sage
19. Fermi M, Chiari F, Mattioli F, et al. Surgical training on ex vivo ovine model in otolaryngology head and neck surgery: a comprehensive review. *Int J Environ Res Public Health*. 2022;19(6):3657. https://pubmed.ncbi.nlm.nih.gov/35329354/
20. Beckmann S, Yacoub A, Fernandez IJ, et al. Exclusive endoscopic laser-stapedotomy: feasibility of an ovine training model. *Otol Neurotol*. 2021;42(7):994-1000. https://pubmed.ncbi.nlm.nih.gov/33935254/
21. Anschuetz L, Bonali M, Ghirelli M, et al. An ovine model for exclusive endoscopic ear surgery. *JAMA Otolaryngol Head Neck Surg*. 2017; 143(3):247-252. https://pubmed.ncbi.nlm.nih.gov/27918787/
22. Fernandez IJ, Bonali M, Yacoub A, et al. Training model for salvage procedures in endoscopic stapes surgery. *Eur Arch Otorhinolaryngol*. 2021;278(4):987-995. https://pubmed.ncbi.nlm.nih.gov/32592010/
23. Uzun GB, Kamaşak B, Ulcay T, Aycan K. Anatomy of parotid gland and it's secretory ducts in sheep. *Folia Morphol (Warsz)*. 2022;81(3): 679-684. https://journals.viamedica.pl/folia_morphologica/article/view/FM.a2021.0071
24. Dehghani SN, Tadjalli M, Masoumzadeh MH. Sialography of sheep parotid and mandibular salivary glands. *Res Vet Sci*. 2000;68(1):3-7.
25. Zenk J, Hosemann WG, Iro H. Diameters of the main excretory ducts of the adult human submandibular and parotid gland: a histologic study. *Oral Surg Oral Med Oral Pathol Oral Radiol Endodontol*. 1998; 85(5):576-580.
26. Vairel B, De Bonnecaze G, Al Shehri S, et al. Courbe d'apprentissage en sialendoscopie: Nos 101 premières procédures. *Rev Laryngol Otol Rhinol*. 2012;133(4–5):177-181. https://pubmed.ncbi.nlm.nih.gov/24006823/
27. Pascoto GR, Stamm AC, Lyra M. Sialendoscopy training: presentation of a realistic model. *Int Arch Otorhinolaryngol*. 2017;21(1):17-20. https://pubmed.ncbi.nlm.nih.gov/28050202/
28. Geisthoff U, Volk GF, Finkensieper M, Wittekindt C, Guntinas-Lichius O. Trainingsmodelle für die Sialendoskopie. *Laryngorhinootologie*. 2015;94(9):587-595.
29. Steck JH, Stabenow E, Volpi EM, Vasconcelos ECG. The learning progression of diagnostic sialendoscopy. *Braz J Otorhinolaryngol*. 2016; 82(2):170-176. https://pubmed.ncbi.nlm.nih.gov/26671021/
30. Anschuetz L, Stricker D, Yacoub A, Wimmer W, Caversaccio M, Huwendiek S. Acquisition of basic ear surgery skills: a randomized comparison between endoscopic and microscopic techniques. *BMC Med Educ*. 2019;19(1):1-9. doi:10.1186/s12909-019-1803-8
31. Saga-Gutierrez C, Chiesa-Estomba CM, Larruscain E, Calvo-Henriquez C, San Jose C, Altuna X. "Omepralith": a novel simulation model for training in sialoendoscopy. *Acta Otorrinolaringol Esp*. 2021; 73(3):137-140. https://pubmed.ncbi.nlm.nih.gov/33814119/

How to cite this article: Borner U, Caversaccio M, Wagner F, Marchal F, Anschuetz L. First evaluation of an ovine training model for sialendoscopy. *Laryngoscope Investigative Otolaryngology*. 2023;8(4):903-911. doi:10.1002/lio2.1116